

Industrial Control

Dynamic event-triggered-based human-in-the-loop formation control for stochastic nonlinear MASs

Yonghua Peng^{1,2}, Guohuai Lin^{1,2,*}, Guangdeng Chen^{1,2}, and Hongyi Li^{1,2}

¹ School of Automation, Guangdong University of Technology, Guangzhou 510006, China

² Guangdong Province Key Laboratory of Intelligent Decision and Cooperative Control, Guangdong University of Technology, Guangzhou 510006, China

Received: 13 April 2023 / Revised: 12 July 2023 / Accepted: 17 August 2023 / Published online: 11 September 2023

Abstract The dynamic event-triggered (DET) formation control problem of a class of stochastic nonlinear multi-agent systems (MASs) with full state constraints is investigated in this article. Supposing that the human operator sends commands to the leader as control input signals, all followers keep formation through network topology communication. Under the command-filter-based backstepping technique, the radial basis function neural networks (RBF NNs) and the barrier Lyapunov function (BLF) are utilized to resolve the problems of unknown nonlinear terms and full state constraints, respectively. Furthermore, a DET control mechanism is proposed to reduce the occupation of communication bandwidth. The presented distributed formation control strategy guarantees that all signals of the MASs are semi-globally uniformly ultimately bounded (SGUUB) in probability. Finally, the feasibility of the theoretical research result is demonstrated by a simulation example.

Keywords Dynamic event-triggered (DET) control, formation control, full state constraints, human-in-the-loop (HiTL), multi agent systems (MASs)

Citation Peng Y, Lin G and Chen G et al. Dynamic event-triggered-based human-in-the-loop formation control for stochastic nonlinear MASs. Security and Safety 2023; 2: 2023024. <https://doi.org/10.1051/sands/2023024>

1 Introduction

In the past decade, with the development of artificial intelligence technology, many effective control strategies have been proposed in the area of cooperative control, such as neural network control, sliding mode control, and fuzzy control [1–6]. In addition, the formation problem of multi-agent systems (MASs) is a significant branch of cooperative control, that has received extensive attention [7]. Formation control in MASs pertains to the coordinated motion of numerous agents in accordance with a predetermined formation pattern, which has found extensive utility in diverse domains such as aerial vehicles, land vehicles, and ships [8–13]. Based on the position of agents, a collaborative control algorithm for auxiliary systems was proposed, which did not require direct measurement of linear velocity to achieve aerial vehicle formation tracking control [9]. It is noteworthy that perturbations in the external environment can substantially impact the accuracy of formation control. For a class of MASs subject to interference, a distributed controller in [10] was formulated to eliminate the influence of the bounded disturbances and optimize the system to reach the intended formation. A robust adaptive controller was developed to effectively minimize the tracking errors of multiple vehicle formation systems with perturbations [11].

* Corresponding authors (email: linguohuai2019@163.com)

Facing the challenge of obstacle avoidance within formation control, a light transmission model was introduced in [12], which improved the traditional artificial potential method. In [13], a dynamic formation tracking control strategy was presented for a class of unmanned aerial vehicles equipped with switching topology to make the drone swarm reach the surrounding area of a designated target.

In recent years, there has been a swift evolution of intelligent control technology for unmanned autonomous systems, which has also garnered the interest of numerous scholars [14–28]. However, there were numerous reported incidents concerning the autonomous control of unmanned systems, which have caused significant negative impacts, prompting concerns and further investigation. In complex environments, enhancing the security of autonomous agent systems is of utmost importance. To improve this, the human-in-the-loop (HiTL) control approaches were analyzed in [29–34], which were proven to be highly effective in enhancing the reliability and security of the system. In light of this background, HiTL control technology has risen rapidly in the field of cooperative control. For the HiTL MASs with time delay, Koru *et al.* [31] proposed an inner loop distributed control method, but it was unsuitable for nonlinear systems. For the HiTL MASs with uncertainty disturbances, a distributed adaptive containment control strategy was presented in [32] to achieve containment control of MASs. In [33], a novel adaptive inverse optimal control method using only state measurement was designed to solve the problem of online adaptive learning human behavior. Lin *et al.* [34] constructed a dynamic model for an unmanned aerial vehicle attitude system and proposed a finite-time command-filtered HiTL control method to achieve a faster convergence rate.

The aforementioned research works have successfully addressed the HiTL control problems. However, the issue of communication network bandwidth is seldom taken into account, which leads to excessive consumption of communication resources. In order to reduce the communication burden, many sampling schemes were proposed [35–45]. For the second-order integral MASs with communication noise, a distributed sampling-data protocol was studied in [46], which solved the average consensus problem. To enable stability for nonlinear systems with sampled-data inputs, Bernuau *et al.* [47] designed a system satisfying a homogeneous condition. It is worth mentioning that the event-triggered-based mechanisms perform with higher resource utilization efficiency than the time-triggered-based mechanisms. In [48], An adaptive control approach was proposed to reduce the communication burden by implementing a fixed threshold event triggering mechanism. In [49, 50], two event-triggered control strategies with relative threshold parameters were considered to further optimize control performance and obtain higher resource utilization efficiency, respectively. It was noteworthy that a novel dynamic event-triggered (DET) strategy was proposed in [51] to solve the network bandwidth problem for a stochastic nonlinear system, which enabled the controller to attain a lower triggering frequency than the traditional sampling control strategy. In addition, Cao *et al.* [52] designed a novel switching DET control mechanism to reduce communication costs.

System states, such as aircraft flight altitude, motor speed, and vehicle turning angle, are often subject to constraints arising from the actual. A system with state constraints is more secure and reliable [53–55]. In [53], a nonlinear state space model of synchronous motors was established to introduce state constraints into the model and guarantee that the motor current was constrained within a certain range. Zhang *et al.* [54] proposed a one-to-one nonlinear mapping strategy, whereby the constrained system is transformed into an unconstrained system, thereby alleviating the burden of state constraints. It is noteworthy that the introduction of the barrier Lyapunov function (BLF) effectively addresses the issue of full-state constraints. For a category of multiple constraint problems, a BLF was designed to handle state constraint problem [55].

Inspired by the above works, a DET formation control strategy is researched for a category of HiTL stochastic nonlinear MASs with full state constraints. The major contributions are outlined below.

- Unlike the formation control of [7–13] where the leader’s output trajectory is given as a reference signal, this paper considers that the leader’s control signal is given by a human operator, which is conducive to realizing the variability of the formation trajectories, with better utility value and safety performance.
- By comparing several time-triggering control and event-triggering control mechanisms [35–52], a DET control mechanism is developed to reduce waste of communication resources between controller and actuator in this paper, which obtains higher resource utilization efficiency.
- The distributed formation controller is developed under the framework of the command filtering backstepping method to achieve formation control, and a filter compensation system is used to handle the

filtering error problem. Furthermore, a BLF is constructed to constrain the states within a certain range, thereby improving the control performance.

2 Preliminaries and problem statement

2.1 Graph theory

MASs exchange information through directed communication topology $\mathcal{G} = (\aleph, \mathcal{M}, \mathcal{Q})$. $\aleph = \{\aleph_1, \aleph_2, \dots, \aleph_N\}$ stands for the point set, $\mathcal{M} = \{(\aleph_i, \aleph_\iota) \in \aleph \times \aleph\}$ represents the edge set, and $\mathcal{Q} = [\rho_{i,\iota}] \in \mathbb{R}^{N \times N}$ means the adjacency matrix, where \aleph_i is the node in the directed communication topology \mathcal{G} , $i = 1, 2, \dots, N$, $\iota = 1, 2, \dots, N$. If $\rho_{i,\iota} = 1$, $(\aleph_i, \aleph_\iota) \in \mathcal{M}$, the follower ι is able to send information to follower i , and if $\rho_{i,\iota} = 0$, $(\aleph_i, \aleph_\iota) \notin \mathcal{M}$ or $i = \iota$. Define $\mathfrak{H} = \text{diag}\{d_1, d_2, \dots, d_N\}$ as the diagonal in-degree matrix and $d_i = \sum_{\iota=1}^N \rho_{i,\iota}$. $F = \mathfrak{H} - \mathcal{Q}$ is described as the graph Laplacian matrix. Define the expansion diagram as $\bar{G} = (\bar{\aleph}, \bar{\mathcal{Q}})$, where $\bar{\aleph} = \{\aleph_0, \aleph_1, \aleph_2, \dots, \aleph_N\}$, \aleph_0 indicates the leader node. $\bar{h}_i = 1$ when the i th follower can receive the leader information, else, $\bar{h}_i = 0$. An expansion diagram adjacency matrix is $\bar{\mathcal{Q}} = [\bar{h}_1, \bar{h}_2, \dots, \bar{h}_N]$.

2.2 Problem statement

The i th ($i = 1, 2, \dots, N$) follower dynamic model is described by

$$\begin{aligned} dx_{i,\vartheta} &= (x_{i,\vartheta+1} + f_{i,\vartheta}(\bar{x}_{i,\vartheta})) dt + g_{i,\vartheta}^T(\bar{x}_{i,\vartheta}) d\omega, \\ dx_{i,n} &= (u_i + f_{i,n}(\bar{x}_{i,n})) dt + g_{i,n}^T(\bar{x}_{i,n}) d\omega, \\ y_i &= x_{i,1}, \quad \vartheta = 1, 2, \dots, n-1 \end{aligned} \quad (1)$$

where $x_{i,\vartheta}$ denotes the systems state with $\vartheta = 1, 2, \dots, n$, $\bar{x}_{i,\vartheta} = [x_{i,1}, x_{i,2}, \dots, x_{i,\vartheta}]^T \in \mathbb{R}^{\vartheta}$, the $f_{i,\vartheta}(\bar{x}_{i,\vartheta}) \in \mathbb{R}$ and $g_{i,\vartheta}(\bar{x}_{i,\vartheta}) \in \mathbb{R}$ represent the unknown nonlinear functions. Assume $g_{i,\vartheta}^T(\bar{x}_{i,\vartheta})$ is bounded. u_i and y_i denote the control input and output of the i th agent, respectively. ω represents an independent q -dimensional Wiener process which is included in a complete probability space $(\Xi, \mathfrak{a}, \{\mathfrak{a}_t\}_{t \geq 0}, \mathcal{J})$, where Ξ represents a sample space, \mathfrak{a} represents a σ -field, \mathfrak{a}_t represents a filtration, \mathcal{J} represents a probability measure.

The leader's input u_0 is supplied by a human operator, which indirectly controls all followers through the network topology, followers can't directly access the information of u_0 . The dynamic model of the leader is considered as

$$\begin{aligned} \dot{x}_{0,1} &= -x_{0,1} + u_0, \\ y_0 &= x_{0,1}, \end{aligned} \quad (2)$$

where $x_{0,1}$ expresses the leader state, y_0 is the leader output.

The main objective of this article is to design a distributed controller where all the agents can maintain a desired formation. All signals in the closed-loop system are bounded in probability and do not violate the full state constraints. To ensure completeness in the design process, the following assumptions and lemmas are made.

Assumption 1. *The leader has at least one directional path to any other node, and the leader output y_0 and its derivative \dot{y}_0 are bounded.*

To enhance the efficiency of communication resources, defining $u_i(t) = u_i$, the DET control mechanism is described as

$$\begin{aligned} u_i(t) &= v_i(\bar{t}_\kappa), \quad t \in [\bar{t}_\kappa, \bar{t}_{\kappa+1}), \\ \bar{t}_{\kappa+1} &= \inf \{t > \bar{t}_\kappa \mid |e_i(t)| \geq \lambda_i(t)|u_i(t)| + \mu_i\}, \\ \dot{\lambda}_i(t) &= -\beta_i \lambda_i^2(t), \end{aligned} \quad (3)$$

where $v_i(\bar{t}_\kappa)$ is the sampled controller input, $e_i(t) = v_i(t) - u_i(t)$, $v_i(t)$ expresses the intermediate continuous control signal, μ_i and β_i are positive parameters. Furthermore, the initial value of $\lambda_i(t)$ satisfies inequality $0 < \lambda_i(0) < 1$. according to (3), it yields

$$u_i(t) = \frac{v_i(t)}{1 + \underline{\mathcal{L}}_i(t)\lambda_i(t)} - \frac{\bar{\mathcal{L}}_i(t)\mu_i}{1 + \underline{\mathcal{L}}_i(t)\lambda_i(t)}, \quad (4)$$

where $\underline{\mathcal{L}}_i(t)$ and $\bar{\mathcal{L}}_i(t)$ are design parameters within the range of $[-1, 1]$.

Lemma 1. [51] Suppose that $d\bar{\delta} = \mathfrak{E}(\bar{\delta}) dt + \mathfrak{D}(\bar{\delta}) d\omega$ expresses a stochastic nonlinear differential equation, where $\bar{\delta} \in \mathbb{R}^n$ represents the system state, $\mathfrak{E}(\bar{\delta})$ and $\mathfrak{D}(\bar{\delta})$ represent the unknown nonlinear functions, ω represents the η -dimensional Wiener process. The corresponding Lyapunov function $V(\bar{\delta}) \in C^2$, the differential operator L of $V(\bar{\delta})$ is given as

$$LV = \frac{\partial V}{\partial \bar{\delta}} \mathfrak{E}(\bar{\delta}) + \frac{1}{2} \text{Tr} \left\{ \mathfrak{D}^T(\bar{\delta}) \frac{\partial^2 V}{\partial \bar{\delta}^2} \mathfrak{D}(\bar{\delta}) \right\}, \quad (5)$$

where $\text{Tr}\{\cdot\}$ expresses a matrix trace.

Assumption 2. The compensation error $z_{i,\vartheta}$ ($\vartheta = 1, 2, \dots, n$) satisfies $|z_{i,\vartheta}| < |E_{i,\vartheta}|$, where $E_{i,\vartheta}$ is a designed constraint parameter for compensation error $z_{i,\vartheta}$.

Lemma 2. [56] The radial basis function neural networks (RBF NNs) $w_{i,\vartheta}^* \phi_{i,\vartheta}(\eta_{i,\vartheta})$ are given to approximate the unknown smooth nonlinear term $\bar{\mathfrak{J}}_{i,\vartheta}(\eta_{i,\vartheta})$

$$\bar{\mathfrak{J}}_{i,\vartheta}(\eta_{i,\vartheta}) = w_{i,\vartheta}^{*T} \phi_{i,\vartheta}(\eta_{i,\vartheta}) + \varrho_{i,\vartheta}, \quad (6)$$

where $\eta_{i,\vartheta}$ indicates the independent variable of the function, $\varrho_{i,\vartheta}$ is the bounded approximation error, $\vartheta = 1, 2, \dots, n$. The ideal weight vector $w_{i,\vartheta}^{*T} \in \mathbb{R}^{\mathfrak{p}}$ is expressed as

$$w_{i,\vartheta}^{*T} = \arg \min_{w_{i,\vartheta}^T \in \Gamma_i} \left\{ \sup_{\eta_{i,\vartheta} \in \wp_i} |\bar{\mathfrak{J}}_{i,\vartheta}(\eta_{i,\vartheta}) - w_{i,\vartheta}^T \phi_{i,\vartheta}(\eta_{i,\vartheta})| \right\},$$

where Γ_i and \wp_i express compact sets of $w_{i,\vartheta}^T$ and $\eta_{i,\vartheta}$, respectively. Define $\mathfrak{R}_{i,\vartheta}^* = \|w_{i,\vartheta}^*\|^2$, $\tilde{\mathfrak{R}}_{i,\vartheta} = \mathfrak{R}_{i,\vartheta}^* - \hat{\mathfrak{R}}_{i,\vartheta}$ with $\hat{\mathfrak{R}}_{i,\vartheta}$ being the estimate of $\mathfrak{R}_{i,\vartheta}^*$. The basis function $\phi_{i,\vartheta}(\eta_{i,\vartheta}) \in \mathbb{R}^{\mathfrak{p}}$ is selected as the following function:

$$\phi_{i,\vartheta}(\eta_{i,\vartheta}) = \exp \left[- \frac{(\eta_{i,\vartheta} - \bar{\zeta}_{i,\vartheta})^T (\eta_{i,\vartheta} - \bar{\zeta}_{i,\vartheta})}{\Psi_{i,\vartheta}} \right],$$

where $\bar{\zeta}_{i,\vartheta}$ and $\Psi_{i,\vartheta}$ represent the center and width of $\phi_{i,\vartheta}(\eta_{i,\vartheta})$, respectively.

Lemma 3. [57] For real variables A and F , the following Young's inequality holds

$$AF \leq \frac{\mathbb{C}}{\mathbb{O}} |A|^{\mathbb{O}} + \frac{1}{\mathbb{U}\mathbb{C}\mathbb{U}} |F|^{\mathbb{U}},$$

where $\mathbb{C} > 0$, $\mathbb{O} > 0$, $\mathbb{U} > 0$, and $(\mathbb{O} - 1)(\mathbb{U} - 1) = 1$.

Lemma 4. [58] The hyperbolic tangent function $\tanh(\mathfrak{k})$ satisfies that $0 \leq |\mathfrak{k}| - \mathfrak{k} \tanh(\frac{\mathfrak{k}}{\delta}) \leq 0.2785\delta$, where $\mathfrak{k} \in \mathbb{R}$ and $\delta > 0$.

3 Controller design

The formation error $s_{i,1}$ ($i = 1, 2, \dots, N$) and error surfaces $s_{i,\vartheta}$ ($\vartheta = 2, 3, \dots, n$) are defined as follows:

$$s_{i,1} = \sum_{\iota=1}^N \rho_{i,\iota} (y_i - y_i - \mathfrak{S}_{i,\iota}) + \bar{h}_i (y_i - y_0 - \mathfrak{S}_{i,0}),$$

$$s_{i,\vartheta} = x_{i,\vartheta} - \partial_{i,\vartheta-1}, \quad (7)$$

where $\mathfrak{S}_{i,\iota}$ and $\mathfrak{S}_{i,0}$ represent the follow i formation distance with follow ι and leader, respectively, $\partial_{i,\vartheta-1}$ represents the command filter output signal, which is constructed as follows:

$$\begin{aligned} \dot{\sigma}_{i,\vartheta 1} &= \xi_{i,\vartheta}, \\ \xi_{i,\vartheta} &= -L_{i,\vartheta} |\sigma_{i,\vartheta 1} - \alpha_{i,\vartheta}|^{\frac{1}{2}} \text{sign}(\sigma_{i,\vartheta 1} - \alpha_{i,\vartheta}) + \sigma_{i,\vartheta 2}, \\ \dot{\sigma}_{i,\vartheta 2} &= -R_{i,\vartheta} \text{sign}(\sigma_{i,\vartheta 2} - \xi_{i,\vartheta}), \end{aligned} \quad (8)$$

where $\alpha_{i,\vartheta}$ is the virtual controller, $\partial_{i,\vartheta} = \sigma_{i,\vartheta 1}$, $L_{i,\vartheta}$ and $R_{i,\vartheta}$ are positive parameters, $\vartheta = 1, 2, \dots, n-1$. The compensating error $z_{i,\vartheta}$ ($\vartheta = 1, 2, \dots, n$) is described as

$$z_{i,\vartheta} = s_{i,\vartheta} - \gamma_{i,\vartheta}, \quad (9)$$

where $\gamma_{i,\vartheta}$ represents the error compensating signal.

The error compensation system is described as

$$\begin{aligned} \dot{\gamma}_{i,1} &= -c_{i,1} \gamma_{i,1} + (d_i + \hbar_i)(\partial_{i,1} - \alpha_{i,1} + \gamma_{i,2}) - k_{i,1} \text{sign}(\gamma_{i,1}), \\ \dot{\gamma}_{i,\vartheta} &= -c_{i,\vartheta} \gamma_{i,\vartheta} + \partial_{i,\vartheta} - \alpha_{i,\vartheta} + \gamma_{i,\vartheta+1} - k_{i,\vartheta} \text{sign}(\gamma_{i,\vartheta}), \\ \dot{\gamma}_{i,n} &= -c_{i,n} \gamma_{i,n} - k_{i,n} \text{sign}(\gamma_{i,n}), \quad \vartheta = 2, 3, \dots, n-1, \end{aligned} \quad (10)$$

where $d_i = \sum_{\iota=1}^N \rho_{i,\iota}$, $c_{i,\vartheta}$ and $k_{i,\vartheta}$ ($\vartheta = 1, 2, \dots, n$) represent positive parameters.

Step 1. According to (1), (2) and (7), the derivative of formation error $s_{i,1}$ is written as

$$\begin{aligned} ds_{i,1} &= \left((d_i + \hbar_i)(x_{i,2} + f_{i,1}(\bar{x}_{i,1})) - \sum_{\iota=1}^N \rho_{i,\iota}(x_{\iota,2} + f_{\iota,1}(\bar{x}_{\iota,1})) - \hbar_i \dot{y}_0 \right) dt \\ &\quad + \left((d_i + \hbar_i) g_{i,1}^T(\bar{x}_{i,1}) - \sum_{\iota=1}^N \rho_{i,\iota} g_{\iota,1}^T(\bar{x}_{\iota,1}) \right) d\omega. \end{aligned} \quad (11)$$

Defining $\mathfrak{T}_{i,1}^T(\Upsilon_{i,1}) = (d_i + \hbar_i) g_{i,1}^T(\bar{x}_{i,1}) - \sum_{\iota=1}^N \rho_{i,\iota} g_{\iota,1}^T(\bar{x}_{\iota,1})$, $\Upsilon_{i,1} = [x_{i,1}, x_{\iota,1}]^T$, and considering (9)–(11), one has

$$\begin{aligned} dz_{i,1} &= \left((d_i + \hbar_i)(z_{i,2} + f_{i,1}(\bar{x}_{i,1}) + \alpha_{i,1}) + c_{i,1} \gamma_{i,1} + k_{i,1} \text{sign}(\gamma_{i,1}) \right. \\ &\quad \left. - \sum_{\iota=1}^N \rho_{i,\iota}(x_{\iota,2} + f_{\iota,1}(\bar{x}_{\iota,1})) - \hbar_i \dot{y}_0 \right) dt + \mathfrak{T}_{i,1}^T(\Upsilon_{i,1}) d\omega. \end{aligned} \quad (12)$$

The BLF is constructed as

$$V_{i,1} = \frac{1}{4} \ln \frac{E_{i,1}^4}{E_{i,1}^4 - z_{i,1}^4} + \frac{\tilde{\mathfrak{R}}_{i,1}^2}{2\tau_{i,1}}, \quad (13)$$

where $|z_{i,1}| < |E_{i,1}|$ with $E_{i,1}$ being the constraint parameter of the compensating error $z_{i,1}$, $\tau_{i,1}$ represents a positive parameter. Combining (12), (13) and Lemma 1, one has

$$\begin{aligned} LV_{i,1} &= \frac{z_{i,1}^3}{E_{i,1}^4 - z_{i,1}^4} \left((d_i + \hbar_i)(z_{i,2} + f_{i,1}(\bar{x}_{i,1}) + \alpha_{i,1}) + c_{i,1} \gamma_{i,1} + k_{i,1} \text{sign}(\gamma_{i,1}) \right. \\ &\quad \left. - \sum_{\iota=1}^N \rho_{i,\iota}(x_{\iota,2} + f_{\iota,1}(\bar{x}_{\iota,1})) - \hbar_i \dot{y}_0 \right) + \frac{z_{i,1}^2 (3E_{i,1}^4 + z_{i,1}^4)}{2(E_{i,1}^4 - z_{i,1}^4)^2} \mathfrak{T}_{i,1}^T(\Upsilon_{i,1}) \mathfrak{T}_{i,1}(\Upsilon_{i,1}) - \frac{\tilde{\mathfrak{R}}_{i,1} \dot{\tilde{\mathfrak{R}}}_{i,1}}{\tau_{i,1}}, \end{aligned} \quad (14)$$

where $\mathfrak{T}_{i,1}(\Upsilon_{i,1})$ has a bounded range. There is a positive parameter $\varrho_{i,1}$ such that $\|\mathfrak{T}_{i,1}(\Upsilon_{i,1})\| \leq \varrho_{i,1}$. By using Lemma 3, the following inequalities hold:

$$\frac{z_{i,1}^3 z_{i,2}}{E_{i,1}^4 - z_{i,1}^4} (d_i + \hbar_i) \leq \frac{z_{i,1}^6}{2(E_{i,1}^4 - z_{i,1}^4)^2} + \frac{z_{i,2}^4}{8} + \frac{(d_i + \hbar_i)^4}{2}, \quad (15)$$

$$\frac{z_{i,1}^3}{E_{i,1}^4 - z_{i,1}^4} k_{i,1} \text{sign}(\gamma_{i,1}) \leq \frac{z_{i,1}^6}{2(E_{i,1}^4 - z_{i,1}^4)^2} + \frac{k_{i,1}^2}{2}, \quad (16)$$

$$\frac{z_{i,1}^2(3E_{i,1}^4 + z_{i,1}^4)}{2(E_{i,1}^4 - z_{i,1}^4)^2} \mathfrak{F}_{i,1}^T(\Upsilon_{i,1}) \mathfrak{F}_{i,1}(\Upsilon_{i,1}) \leq \frac{z_{i,1}^4(3E_{i,1}^4 + z_{i,1}^4)^2}{8(E_{i,1}^4 - z_{i,1}^4)^4} + \frac{\mathcal{D}_{i,1}^4}{2}. \quad (17)$$

Substituting (15)–(17) into (14), $LV_{i,1}$ can be rewritten as

$$\begin{aligned} LV_{i,1} \leq & \frac{z_{i,1}^3}{E_{i,1}^4 - z_{i,1}^4} \left((d_i + \bar{h}_i)(f_{i,1}(\bar{x}_{i,1}) + \alpha_{i,1}) + c_{i,1}\gamma_{i,1} - \sum_{i=1}^N \rho_{i,\iota}(x_{i,2} + f_{i,1}(\bar{x}_{i,1})) - \bar{h}_i \dot{y}_0 \right) \\ & + \frac{\mathcal{D}_{i,1}^4}{2} + \frac{z_{i,1}^6}{(E_{i,1}^4 - z_{i,1}^4)^2} + \frac{z_{i,1}^4}{8} + \frac{(d_i + \bar{h}_i)^4}{2} + \frac{k_{i,1}^2}{2} + \frac{z_{i,1}^4(3E_{i,1}^4 + z_{i,1}^4)^2}{8(E_{i,1}^4 - z_{i,1}^4)^4} - \frac{\mathfrak{H}_{i,1} \dot{\mathfrak{H}}_{i,1}}{\tau_{i,1}}. \end{aligned} \quad (18)$$

A nonlinear function $\bar{\mathfrak{J}}_{i,1}(\eta_{i,1})$ is described as

$$\bar{\mathfrak{J}}_{i,1}(\eta_{i,1}) = (d_i + \bar{h}_i)f_{i,1}(\bar{x}_{i,1}) - \bar{h}_i \dot{y}_0 + \frac{z_{i,1}(3E_{i,1}^4 + z_{i,1}^4)^2}{8(E_{i,1}^4 - z_{i,1}^4)^3} - \sum_{i=1}^N \rho_{i,\iota}(x_{i,2} + f_{i,1}(\bar{x}_{i,1})) \quad (19)$$

where $\eta_{i,1} = [x_{i,1}, x_{i,2}, x_{i,2}]^T$. By using Lemmas 2 and 3, there is a positive parameter $\bar{\varrho}_{i,1}$ such that $|\varrho_{i,1}| \leq \bar{\varrho}_{i,1}$, one has

$$\frac{z_{i,1}^3}{E_{i,1}^4 - z_{i,1}^4} \bar{\mathfrak{J}}_{i,1}(\eta_{i,1}) \leq \frac{z_{i,1}^6}{2(E_{i,1}^4 - z_{i,1}^4)^2} + \frac{\bar{\varrho}_{i,1}^2}{2} + \frac{\epsilon_{i,1}^2}{2} + \frac{z_{i,1}^6 \mathfrak{R}_{i,1}^* \phi_{i,1}^T(\eta_{i,1}) \phi_{i,1}(\eta_{i,1})}{2(E_{i,1}^4 - z_{i,1}^4)^2 \epsilon_{i,1}^2}, \quad (20)$$

where $\epsilon_{i,1}$ is a design parameter.

The virtual controller $\alpha_{i,1}$ and adaptive law $\dot{\mathfrak{H}}_{i,1}$ are designed as

$$\alpha_{i,1} = -\frac{z_{i,1}^3 \hat{\mathfrak{H}}_{i,1} \phi_{i,1}^T(\eta_{i,1}) \phi_{i,1}(\eta_{i,1})}{2(d_i + \bar{h}_i)(E_{i,1}^4 - z_{i,1}^4) \epsilon_{i,1}^2} - \frac{c_{i,1} s_{i,1}}{d_i + \bar{h}_i} - \frac{3z_{i,1}^3}{2(E_{i,1}^4 - z_{i,1}^4)(d_i + \bar{h}_i)}, \quad (21)$$

$$\dot{\mathfrak{H}}_{i,1} = \frac{\tau_{i,1} z_{i,1}^6 \phi_{i,1}^T(\eta_{i,1}) \phi_{i,1}(\eta_{i,1})}{2(E_{i,1}^4 - z_{i,1}^4)^2 \epsilon_{i,1}^2} - H_{i,1} \hat{\mathfrak{H}}_{i,1}, \quad (22)$$

where $H_{i,1}$ is a positive parameter. Combining (18)–(22), we can obtain that

$$LV_{i,1} \leq -\frac{c_{i,1} z_{i,1}^4}{E_{i,1}^4 - z_{i,1}^4} + \frac{z_{i,1}^4}{8} + \frac{(d_i + \bar{h}_i)^4}{2} + \frac{\bar{\varrho}_{i,1}^2}{2} + \frac{\epsilon_{i,1}^2}{2} + \frac{k_{i,1}^2}{2} + \frac{\mathcal{D}_{i,1}^4}{2} + \frac{H_{i,1} \mathfrak{H}_{i,1} \dot{\mathfrak{H}}_{i,1}}{\tau_{i,1}}. \quad (23)$$

Step ϑ ($\vartheta = 2, 3, \dots, n - 1$). From (1) and (7), one has

$$ds_{i,\vartheta} = (x_{i,\vartheta+1} + f_{i,\vartheta}(\bar{x}_{i,\vartheta}) - \dot{\hat{\delta}}_{i,\vartheta-1}) dt + g_{i,\vartheta}^T(\bar{x}_{i,\vartheta}) d\omega. \quad (24)$$

Using (9), (10) and (24), it yields

$$dz_{i,\vartheta} = (z_{i,\vartheta+1} + f_{i,\vartheta}(\bar{x}_{i,\vartheta}) + \alpha_{i,\vartheta} + c_{i,\vartheta}\gamma_{i,\vartheta} + k_{i,\vartheta} \text{sign}(\gamma_{i,\vartheta}) - \dot{\hat{\delta}}_{i,\vartheta-1}) dt + g_{i,\vartheta}^T(\bar{x}_{i,\vartheta}) d\omega \quad (25)$$

where $g_{i,\vartheta}^T(\bar{x}_{i,\vartheta})$ has a bounded range. There is a positive parameter $\mathcal{D}_{i,\vartheta}$ such that $\|g_{i,\vartheta}^T(\bar{x}_{i,\vartheta})\| \leq \mathcal{D}_{i,\vartheta}$.

The BLF is constructed as

$$V_{i,\vartheta} = V_{i,\vartheta-1} + \frac{1}{4} \ln \frac{E_{i,\vartheta}^4}{E_{i,\vartheta}^4 - z_{i,\vartheta}^4} + \frac{\hat{\mathfrak{H}}_{i,\vartheta}^2}{2\tau_{i,\vartheta}}, \quad (26)$$

where $|z_{i,\vartheta}| < |E_{i,\vartheta}|$ with $E_{i,\vartheta}$ being the constraint parameter of the compensating error $z_{i,\vartheta}$, $\tau_{i,\vartheta}$ is a positive parameter. Combining (25), (26) and Lemma 1, one has

$$\begin{aligned} LV_{i,\vartheta} \leq & LV_{i,\vartheta-1} + \frac{z_{i,\vartheta}^3}{E_{i,\vartheta}^4 - z_{i,\vartheta}^4} (z_{i,\vartheta+1} + f_{i,\vartheta}(\bar{x}_{i,\vartheta}) + \alpha_{i,\vartheta} + c_{i,\vartheta}\gamma_{i,\vartheta} + k_{i,\vartheta} \text{sign}(\gamma_{i,\vartheta}) - \dot{\delta}_{i,\vartheta-1}) \\ & + \frac{z_{i,\vartheta}^2 (3E_{i,\vartheta}^4 + z_{i,\vartheta}^4)}{2(E_{i,\vartheta}^4 - z_{i,\vartheta}^4)^2} \vartheta_{i,\vartheta}^2 - \frac{\tilde{\mathfrak{R}}_{i,\vartheta} \dot{\mathfrak{R}}_{i,\vartheta}}{\tau_{i,\vartheta}}, \end{aligned} \quad (27)$$

From Lemma 3, the following inequalities hold:

$$\frac{z_{i,\vartheta}^3}{E_{i,\vartheta}^4 - z_{i,\vartheta}^4} z_{i,\vartheta+1} \leq \frac{z_{i,\vartheta}^6}{2(E_{i,\vartheta}^4 - z_{i,\vartheta}^4)^2} + \frac{z_{i,\vartheta+1}^4}{8} + \frac{1}{2}, \quad (28)$$

$$\frac{z_{i,\vartheta}^3}{E_{i,\vartheta}^4 - z_{i,\vartheta}^4} k_{i,\vartheta} \text{sign}(\gamma_{i,\vartheta}) \leq \frac{z_{i,\vartheta}^6}{2(E_{i,\vartheta}^4 - z_{i,\vartheta}^4)^2} + \frac{k_{i,\vartheta}^2}{2}, \quad (29)$$

$$\frac{z_{i,\vartheta}^2 (3E_{i,\vartheta}^4 + z_{i,\vartheta}^4)}{2(E_{i,\vartheta}^4 - z_{i,\vartheta}^4)^2} \vartheta_{i,\vartheta}^2 \leq \frac{\vartheta_{i,\vartheta}^4}{2} + \frac{z_{i,\vartheta}^4 (3E_{i,\vartheta}^4 + z_{i,\vartheta}^4)^2}{8(E_{i,\vartheta}^4 - z_{i,\vartheta}^4)^4}. \quad (30)$$

Substituting (28)–(30) into (27), it yields

$$\begin{aligned} LV_{i,\vartheta} \leq & LV_{i,\vartheta-1} + \frac{z_{i,\vartheta}^3}{E_{i,\vartheta}^4 - z_{i,\vartheta}^4} (f_{i,\vartheta}(\bar{x}_{i,\vartheta}) + \alpha_{i,\vartheta} + c_{i,\vartheta}\gamma_{i,\vartheta} - \dot{\delta}_{i,\vartheta-1}) + \frac{z_{i,\vartheta}^6}{(E_{i,\vartheta}^4 - z_{i,\vartheta}^4)^2} \\ & + \frac{z_{i,\vartheta+1}^4}{8} + \frac{z_{i,\vartheta}^4 (3E_{i,\vartheta}^4 + z_{i,\vartheta}^4)^2}{8(E_{i,\vartheta}^4 - z_{i,\vartheta}^4)^4} + \frac{\vartheta_{i,\vartheta}^4}{2} + \frac{k_{i,\vartheta}^2}{2} + \frac{1}{2} - \frac{\tilde{\mathfrak{R}}_{i,\vartheta} \dot{\mathfrak{R}}_{i,\vartheta}}{\tau_{i,\vartheta}}. \end{aligned} \quad (31)$$

A nonlinear function $\tilde{\mathfrak{J}}_{i,\vartheta}(\eta_{i,\vartheta})$ is defined as

$$\tilde{\mathfrak{J}}_{i,\vartheta}(\eta_{i,\vartheta}) = f_{i,\vartheta}(\bar{x}_{i,\vartheta}) + \frac{z_{i,\vartheta} (3E_{i,\vartheta}^4 + z_{i,\vartheta}^4)^2}{8(E_{i,\vartheta}^4 - z_{i,\vartheta}^4)^3} \quad (32)$$

where $\eta_{i,\vartheta} = [x_{i,1}, x_{i,2}, \dots, x_{i,\vartheta}]^T$. By using Lemmas 2 and 3, there is a positive constant $\bar{\varrho}_{i,\vartheta}$ such that $|\varrho_{i,\vartheta}| \leq \bar{\varrho}_{i,\vartheta}$, one has

$$\frac{z_{i,\vartheta}^3}{E_{i,\vartheta}^4 - z_{i,\vartheta}^4} \tilde{\mathfrak{J}}_{i,\vartheta}(\eta_{i,\vartheta}) \leq \frac{z_{i,\vartheta}^6}{2(E_{i,\vartheta}^4 - z_{i,\vartheta}^4)^2} + \frac{\bar{\varrho}_{i,\vartheta}^2}{2} + \frac{\epsilon_{i,\vartheta}^2}{2} + \frac{z_{i,\vartheta}^6 \mathfrak{R}_{i,\vartheta}^* \phi_{i,\vartheta}^T(\eta_{i,\vartheta}) \phi_{i,\vartheta}(\eta_{i,\vartheta})}{2(E_{i,\vartheta}^4 - z_{i,\vartheta}^4)^2 \epsilon_{i,\vartheta}^2}, \quad (33)$$

where $\epsilon_{i,\vartheta}$ expresses a design parameter.

The virtual controller $\alpha_{i,\vartheta}$ and adaptive law $\dot{\mathfrak{R}}_{i,\vartheta}$ are designed as

$$\alpha_{i,\vartheta} = -c_{i,\vartheta} s_{i,\vartheta} - \frac{z_{i,\vartheta}^3 \hat{\mathfrak{R}}_{i,\vartheta} \phi_{i,\vartheta}^T(\eta_{i,\vartheta}) \phi_{i,\vartheta}(\eta_{i,\vartheta})}{2(E_{i,\vartheta}^4 - z_{i,\vartheta}^4) \epsilon_{i,\vartheta}^2} - \frac{3z_{i,\vartheta}^3}{2(E_{i,\vartheta}^4 - z_{i,\vartheta}^4)} - \frac{(E_{i,\vartheta}^4 - z_{i,\vartheta}^4)}{8} z_{i,\vartheta} + \dot{\delta}_{i,\vartheta-1}, \quad (34)$$

$$\dot{\mathfrak{R}}_{i,\vartheta} = \frac{\tau_{i,\vartheta} z_{i,\vartheta}^6 \phi_{i,\vartheta}^T(\eta_{i,\vartheta}) \phi_{i,\vartheta}(\eta_{i,\vartheta})}{2(E_{i,\vartheta}^4 - z_{i,\vartheta}^4)^2 \epsilon_{i,\vartheta}^2} - H_{i,\vartheta} \hat{\mathfrak{R}}_{i,\vartheta}, \quad (35)$$

where $H_{i,\vartheta}$ is a positive parameter. Based on (31)–(35) and (23), we can know

$$\begin{aligned} LV_{i,\vartheta} \leq & \sum_{m=1}^{\vartheta} \left(-\frac{c_{i,m} z_{i,m}^4}{E_{i,m}^4 - z_{i,m}^4} + \frac{\epsilon_{i,m}^2}{2} + \frac{k_{i,m}^2}{2} + \frac{\vartheta_{i,m}^4}{2} + \frac{\bar{\varrho}_{i,m}^2}{2} + \frac{H_{i,m} \tilde{\mathfrak{R}}_{i,m} \hat{\mathfrak{R}}_{i,m}}{\tau_{i,m}} \right) \\ & + \frac{(d_i + \bar{h}_i)^4}{2} + \frac{z_{i,\vartheta+1}^4}{8} + \frac{\vartheta - 1}{2}. \end{aligned} \quad (36)$$

Step n. Similar to previous steps, according to (1) and (7), the derivative of $s_{i,n}$ is given as

$$ds_{i,n} = (u_i + f_{i,n}(\bar{x}_{i,n}) - \dot{\delta}_{i,n-1}) dt + g_{i,n}^T(\bar{x}_{i,n}) d\omega. \quad (37)$$

According to (9), (10) and (37), we can know

$$dz_{i,n} = (u_i + f_{i,n}(\bar{x}_{i,n}) - \dot{\delta}_{i,n-1} + c_{i,n}\gamma_{i,n} + k_{i,n} \text{sign}(\gamma_{i,n})) dt + g_{i,n}^T(\bar{x}_{i,n}) d\omega \quad (38)$$

where $g_{i,n}^T(\bar{x}_{i,n})$ has a bounded range. There is a positive parameter $\varrho_{i,n}$ such that $\|g_{i,n}^T(\bar{x}_{i,n})\| \leq \varrho_{i,n}$. Then, the BLF is defined as

$$V_{i,n} = V_{i,n-1} + \frac{1}{4} \ln \frac{E_{i,n}^4}{E_{i,n}^4 - z_{i,n}^4} + \frac{\tilde{\mathfrak{R}}_{i,n}^2}{2\tau_{i,n}}, \quad (39)$$

where $|z_{i,n}| < |E_{i,n}|$ with $E_{i,n}$ being the constraint parameter of the compensating error $z_{i,n}$, $\tau_{i,n}$ is a positive parameter. Combining (38), (39) and Lemma 1, one has

$$\begin{aligned} LV_{i,n} &\leq LV_{i,n-1} + \frac{z_{i,n}^3}{E_{i,n}^4 - z_{i,n}^4} (f_{i,n}(\bar{x}_{i,n}) + c_{i,n}\gamma_{i,n} + k_{i,n} \text{sign}(\gamma_{i,n}) + u_i - \dot{\delta}_{i,n-1}) \\ &\quad + \frac{z_{i,n}^2 (3E_{i,n}^4 + z_{i,n}^4)}{2(E_{i,n}^4 - z_{i,n}^4)^2} \varrho_{i,n}^2 - \frac{\tilde{\mathfrak{R}}_{i,n} \dot{\mathfrak{R}}_{i,n}}{\tau_{i,n}}. \end{aligned} \quad (40)$$

Substituting (4) into (40), it yields

$$\begin{aligned} LV_{i,n} &\leq LV_{i,n-1} + \frac{z_{i,n}^3}{E_{i,n}^4 - z_{i,n}^4} \left(f_{i,n}(\bar{x}_{i,n}) - \dot{\delta}_{i,n-1} + c_{i,n}\gamma_{i,n} + k_{i,n} \text{sign}(\gamma_{i,n}) + \frac{v_i(t)}{1 + \underline{\mathcal{L}}_i(t)\lambda_i(t)} \right. \\ &\quad \left. - \frac{\bar{\mathcal{L}}_i \mu_i}{1 + \underline{\mathcal{L}}_i(t)\lambda_i(t)} \right) + \frac{z_{i,n}^2 (3E_{i,n}^4 + z_{i,n}^4)}{2(E_{i,n}^4 - z_{i,n}^4)^2} \varrho_{i,n}^2 - \frac{\tilde{\mathfrak{R}}_{i,n} \dot{\mathfrak{R}}_{i,n}}{\tau_{i,n}}. \end{aligned} \quad (41)$$

$v_i(t)$ is constructed as

$$v_i(t) = -(1 + \lambda_i(t)) \left(\alpha_{i,n} \tanh \left(\frac{z_{i,n}^3 \alpha_{i,n}}{\delta_i (E_{i,n}^4 - z_{i,n}^4)} \right) + \varphi_{i,n} \tanh \left(\frac{z_{i,n}^3 \varphi_{i,n}}{\delta_i (E_{i,n}^4 - z_{i,n}^4)} \right) \right), \quad (42)$$

where δ_i and $\varphi_{i,n}$ are positive parameters with $\varphi_{i,n} > \frac{\mu_i}{1 - \lambda_i(t)}$. Because $\underline{\mathcal{L}}_i(t)$ and $\bar{\mathcal{L}}_i(t)$ are design parameters within the range of $[-1, 1]$, we have

$$\frac{z_{i,n}^3 v_i(t)}{(E_{i,n}^4 - z_{i,n}^4)(1 + \underline{\mathcal{L}}_i(t)\lambda_i(t))} \leq \frac{z_{i,n}^3 v_i(t)}{(E_{i,n}^4 - z_{i,n}^4)(1 + \lambda_i(t))}, \quad (43)$$

$$-\frac{z_{i,n}^3 \bar{\mathcal{L}}_i \mu_i}{(E_{i,n}^4 - z_{i,n}^4)(1 + \underline{\mathcal{L}}_i(t)\lambda_i(t))} \leq \frac{|z_{i,n}^3| \mu_i}{(E_{i,n}^4 - z_{i,n}^4)(1 - \lambda_i(t))}. \quad (44)$$

Substituting (42)–(44) into (41), we can get

$$\begin{aligned} LV_{i,n} &\leq LV_{i,n-1} + \frac{z_{i,n}^3}{E_{i,n}^4 - z_{i,n}^4} \left(f_{i,n}(\bar{x}_{i,n}) + c_{i,n}\gamma_{i,n} - \dot{\delta}_{i,n-1} - \alpha_{i,n} \tanh \left(\frac{z_{i,n}^3 \alpha_{i,n}}{\delta_i (E_{i,n}^4 - z_{i,n}^4)} \right) \right. \\ &\quad \left. + k_{i,n} \text{sign}(\gamma_{i,n}) - \varphi_{i,n} \tanh \left(\frac{z_{i,n}^3 \varphi_{i,n}}{\delta_i (E_{i,n}^4 - z_{i,n}^4)} \right) \right) + \frac{|z_{i,n}^3| \mu_i}{(E_{i,n}^4 - z_{i,n}^4)(1 - \lambda_i(t))} \\ &\quad + \frac{z_{i,n}^2 (3E_{i,n}^4 + z_{i,n}^4)}{2(E_{i,n}^4 - z_{i,n}^4)^2} \varrho_{i,n}^2 - \frac{\tilde{\mathfrak{R}}_{i,n} \dot{\mathfrak{R}}_{i,n}}{\tau_{i,n}}. \end{aligned} \quad (45)$$

From Lemma 4, we have

$$-\frac{z_{i,n}^3 \alpha_{i,n}}{(E_{i,n}^4 - z_{i,n}^4)} \tanh\left(\frac{z_{i,n}^3 \alpha_{i,n}}{\delta_i (E_{i,n}^4 - z_{i,n}^4)}\right) \leq -\left|\frac{z_{i,n}^3 \alpha_{i,n}}{(E_{i,n}^4 - z_{i,n}^4)}\right| + 0.2785\delta_i, \quad (46)$$

$$-\frac{z_{i,n}^3 \varphi_{i,n}}{(E_{i,n}^4 - z_{i,n}^4)} \tanh\left(\frac{z_{i,n}^3 \varphi_{i,n}}{\delta_i (E_{i,n}^4 - z_{i,n}^4)}\right) \leq -\left|\frac{z_{i,n}^3 \varphi_{i,n}}{(E_{i,n}^4 - z_{i,n}^4)}\right| + 0.2785\delta_i. \quad (47)$$

Then, combining (45)–(47), it yields

$$\begin{aligned} LV_{i,n} \leq & LV_{i,n-1} + \frac{z_{i,n}^3}{E_{i,n}^4 - z_{i,n}^4} \left(f_{i,n}(\bar{x}_{i,n}) + \alpha_{i,n} + c_{i,n}\gamma_{i,n} + k_{i,n} \operatorname{sign}(\gamma_{i,n}) - \dot{\delta}_{i,n-1} \right) \\ & + \frac{|z_{i,n}^3| \mu_i}{(E_{i,n}^4 - z_{i,n}^4)(1 - \lambda_i(t))} + 0.557\delta_i + \frac{z_{i,n}^2 (3E_{i,n}^4 + z_{i,n}^4)}{2(E_{i,n}^4 - z_{i,n}^4)^2} \mathcal{D}_{i,n}^2 - \frac{\tilde{\mathfrak{R}}_{i,n} \dot{\mathfrak{R}}_{i,n}}{\tau_{i,n}}. \end{aligned} \quad (48)$$

By using Lemma 3, we have

$$\frac{z_{i,n}^3}{E_{i,n}^4 - z_{i,n}^4} k_{i,n} \operatorname{sign}(\gamma_{i,n}) \leq \frac{z_{i,n}^6}{2(E_{i,n}^4 - z_{i,n}^4)^2} + \frac{k_{i,n}^2}{2}, \quad (49)$$

$$\frac{z_{i,n}^2 (3E_{i,n}^4 + z_{i,n}^4)}{2(E_{i,n}^4 - z_{i,n}^4)^2} \mathcal{D}_{i,n}^2 \leq \frac{\mathcal{D}_{i,n}^4}{2} + \frac{z_{i,n}^4 (3E_{i,n}^4 + z_{i,n}^4)^2}{8(E_{i,n}^4 - z_{i,n}^4)^4}, \quad (50)$$

$$\frac{\mu_i |z_{i,n}^3|}{(1 - \lambda_i(t))(E_{i,n}^4 - z_{i,n}^4)} \leq \frac{\mu_i^2}{2(1 - \lambda_i(t))^2} + \frac{z_{i,n}^6}{2(E_{i,n}^4 - z_{i,n}^4)^2}. \quad (51)$$

Substituting (49)–(51) into (48), one has

$$\begin{aligned} LV_{i,n} \leq & LV_{i,n-1} + \frac{z_{i,n}^3}{E_{i,n}^4 - z_{i,n}^4} (\alpha_{i,n} + f_{i,n}(\bar{x}_{i,n}) + c_{i,n}\gamma_{i,n} - \dot{\delta}_{i,n-1}) + \frac{z_{i,n}^6}{(E_{i,n}^4 - z_{i,n}^4)^2} + \frac{\mu_i^2}{2(1 - \lambda_i(t))^2} \\ & + 0.557\delta_i + \frac{k_{i,n}^2}{2} + \frac{\mathcal{D}_{i,n}^4}{2} + \frac{z_{i,n}^4 (3E_{i,n}^4 + z_{i,n}^4)^2}{8(E_{i,n}^4 - z_{i,n}^4)^4} - \frac{\tilde{\mathfrak{R}}_{i,n} \dot{\mathfrak{R}}_{i,n}}{\tau_{i,n}}. \end{aligned} \quad (52)$$

A nonlinear function $\tilde{\mathfrak{J}}_{i,n}(\eta_{i,n})$ is defined as

$$\tilde{\mathfrak{J}}_{i,n}(\eta_{i,n}) = f_{i,n}(\bar{x}_{i,n}) + \frac{z_{i,n} (3E_{i,n}^4 + z_{i,n}^4)^2}{8(E_{i,n}^4 - z_{i,n}^4)^3} \quad (53)$$

where $\eta_{i,n} = [x_{i,1}, x_{i,2}, \dots, x_{i,n}]^T$, By using Lemmas 2 and 3, there is a positive parameter $\bar{\varrho}_{i,n}$ such that $|\varrho_{i,n}| \leq \bar{\varrho}_{i,n}$, it yields

$$\frac{z_{i,n}^3}{E_{i,n}^4 - z_{i,n}^4} \tilde{\mathfrak{J}}_{i,n}(\eta_{i,n}) \leq \frac{z_{i,n}^6}{2(E_{i,n}^4 - z_{i,n}^4)^2} + \frac{\bar{\varrho}_{i,n}^2}{2} + \frac{\epsilon_{i,n}^2}{2} + \frac{z_{i,n}^6 \mathfrak{R}_{i,n}^* \phi_{i,n}^T(\eta_{i,n}) \phi_{i,n}(\eta_{i,n})}{2(E_{i,n}^4 - z_{i,n}^4)^2 \epsilon_{i,n}^2}, \quad (54)$$

where $\epsilon_{i,n}$ represents a design parameter.

The virtual controller $\alpha_{i,n}$ and adaptive law $\dot{\mathfrak{R}}_{i,n}$ are designed as

$$\alpha_{i,n} = -c_{i,n}s_{i,n} - \frac{z_{i,n}^3 \hat{\mathfrak{R}}_{i,n} \phi_{i,n}^T(\eta_{i,n}) \phi_{i,n}(\eta_{i,n})}{2(E_{i,n}^4 - z_{i,n}^4) \epsilon_{i,n}^2} - \frac{3z_{i,n}^3}{2(E_{i,n}^4 - z_{i,n}^4)} - \frac{(E_{i,n}^4 - z_{i,n}^4)}{8} z_{i,n} + \dot{\delta}_{i,n-1}, \quad (55)$$

$$\dot{\mathfrak{R}}_{i,n} = \frac{\tau_{i,n} z_{i,n}^6 \phi_{i,n}^T(\eta_{i,n}) \phi_{i,n}(\eta_{i,n})}{2(E_{i,n}^4 - z_{i,n}^4)^2 \epsilon_{i,n}^2} - H_{i,n} \hat{\mathfrak{R}}_{i,n}, \quad (56)$$

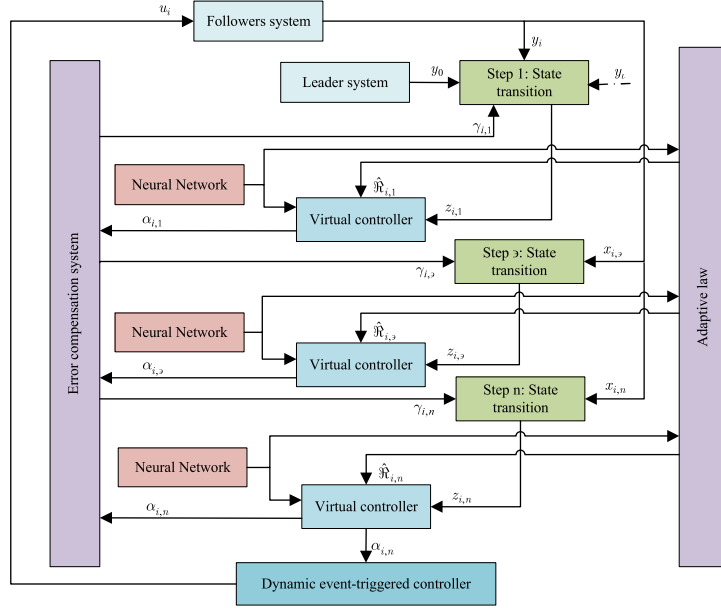


Figure 1. The block diagram of the distributed formation control

where $H_{i,n}$ is a positive parameter.

According to (3), we can know $0 < \lambda_i(0) < 1$ and $\dot{\lambda}_i(t) = -\beta_i \lambda_i^2(t)$, β_i is a positive parameter, so there has a positive parameter $\bar{\mu}_i$ with $\frac{\mu_i^2}{2(1-\lambda_i(t))^2} < \bar{\mu}_i$. Combining (52)–(56) and (36), defining $D_i = \sum_{\vartheta=1}^n \frac{\bar{g}_{i,\vartheta}^2}{2} + \sum_{\vartheta=1}^n \frac{\bar{\epsilon}_{i,\vartheta}^2}{2} + \sum_{\vartheta=1}^n \frac{\bar{k}_{i,\vartheta}^2}{2} + \sum_{\vartheta=1}^n \frac{\bar{\varrho}_{i,\vartheta}^4}{2} + \bar{\mu}_i + 0.557\delta_i + \frac{(d_i+h_i)^4}{2} + \frac{n-2}{2}$, then we have

$$LV_{i,n} \leq - \sum_{\vartheta=1}^n \frac{c_{i,\vartheta} z_{i,\vartheta}^4}{E_{i,\vartheta}^4 - z_{i,\vartheta}^4} + \sum_{\vartheta=1}^n \frac{H_{i,\vartheta} \tilde{\mathfrak{R}}_{i,\vartheta} \hat{\mathfrak{R}}_{i,\vartheta}}{\tau_{i,\vartheta}} + D_i. \quad (57)$$

According to the above description, the block diagram of a distributed formation controller based on DET for HiTL stochastic MASs is shown in Figure 1.

4 Stability analysis

Theorem 1. For the MASs (1) with full state constraints, based on (5), (6), incorporating the DET mechanism (3), the virtual controllers (21), (34) and (55), the adaptive laws (22), (35) and (56), and the intermediate control signal (45) are constructed, then the DET formation controller guarantees that all signals in the MASs are semi-globally uniformly ultimately bounded (SGUUB) in probability.

Proof. A Lyapunov function is constructed as

$$V = \sum_{i=1}^N V_{i,n}. \quad (58)$$

According to Lemmas 2 and 3, one has

$$\frac{H_{i,\vartheta} \tilde{\mathfrak{R}}_{i,\vartheta} \hat{\mathfrak{R}}_{i,\vartheta}}{\tau_{i,\vartheta}} \leq -\frac{H_{i,\vartheta} \tilde{\mathfrak{R}}_{i,\vartheta}^2}{2\tau_{i,\vartheta}} + \frac{H_{i,\vartheta} \mathfrak{R}_{i,\vartheta}^{*2}}{2\tau_{i,\vartheta}} \quad (59)$$

where $\vartheta = 1, 2, \dots, n$. Substituting (57) and (59) into (58), one has

$$LV \leq \sum_{i=1}^N \sum_{\vartheta=1}^n \left(-\frac{c_{i,\vartheta} z_{i,\vartheta}^4}{E_{i,\vartheta}^4 - z_{i,\vartheta}^4} - \frac{H_{i,\vartheta} \tilde{\mathfrak{R}}_{i,\vartheta}^2}{2\tau_{i,\vartheta}} + \frac{H_{i,\vartheta} \mathfrak{R}_{i,\vartheta}^{*2}}{2\tau_{i,\vartheta}} \right) + \sum_{i=1}^N D_i. \quad (60)$$

According to the definition of $V_{i,\vartheta}$, yields $-\frac{c_{i,\vartheta}z_{i,\vartheta}^4}{E_{i,\vartheta}^4 - z_{i,\vartheta}^4} \leq -c_{i,\vartheta} \ln \frac{E_{i,\vartheta}^4}{E_{i,\vartheta}^4 - z_{i,\vartheta}^4}$, one has

$$LV \leq \sum_{i=1}^N \sum_{\vartheta=1}^n \left(-c_{i,\vartheta} \ln \frac{E_{i,\vartheta}^4}{E_{i,\vartheta}^4 - z_{i,\vartheta}^4} - \frac{H_{i,\vartheta} \tilde{\mathfrak{R}}_{i,\vartheta}^2}{2\tau_{i,\vartheta}} + \frac{H_{i,\vartheta} \mathfrak{R}_{i,\vartheta}^{*2}}{2\tau_{i,\vartheta}} \right) + \sum_{i=1}^N D_i. \quad (61)$$

Then, one has

$$\frac{dE(V(t))}{dt} \leq -C_1 E(V(t)) + C_2, \quad (62)$$

where $C_1 = \min\{4c_{i,\vartheta}, H_{i,\vartheta}\}$ and $C_2 = \sum_{i=1}^N D_i + \sum_{i=1}^N \sum_{\vartheta=1}^n \frac{H_{i,\vartheta} \mathfrak{R}_{i,\vartheta}^{*2}}{2\tau_{i,\vartheta}}$. Finding the integral of (62), we can know

$$0 \leq E(V(t)) \leq \left(V(0) - \frac{C_2}{C_1} \right) e^{-C_1 t} + \frac{C_2}{C_1}. \quad (63)$$

From (63), by designing appropriate initial values and parameters, all signals in MASs are SGUUB in probability.

Zeno behavior will occur if the event is triggered infinitely in a limited time. The following proof demonstrates the exclusion of Zeno behavior. The derivative of $|e_i(t)|$ is given as

$$\frac{d}{dt} |e_i(t)| = \frac{d}{dt} (e_i(t) e_i(t))^{\frac{1}{2}} = \dot{e}_i(t) \operatorname{sign}(e_i(t)) \leq |\dot{v}_i(t)|, \quad (64)$$

where $t \in [\bar{t}_\kappa, \bar{t}_{\kappa+1})$. According to (3) and (42), it yields

$$\begin{aligned} \dot{v}_i(t) &= \beta_i \lambda_i^2(t) \left(\alpha_{i,n} \tanh \left(\frac{z_{i,n}^3 \alpha_{i,n}}{\delta_i (E_{i,n}^4 - z_{i,n}^4)} \right) + \varphi_{i,n} \tanh \left(\frac{z_{i,n}^3 \varphi_{i,n}}{\delta_i (E_{i,n}^4 - z_{i,n}^4)} \right) \right) - (1 + \lambda_i(t)) \\ &\times \left(\dot{\alpha}_{i,n} \tanh \left(\frac{z_{i,n}^3 \alpha_{i,n}}{\delta_i (E_{i,n}^4 - z_{i,n}^4)} \right) + \frac{z_{i,n}^3 \dot{\alpha}_{i,n} \alpha_{i,n}}{\delta_i (E_{i,n}^4 - z_{i,n}^4) \cosh^2 \left(\frac{z_{i,n}^3 \alpha_{i,n}}{\delta_i (E_{i,n}^4 - z_{i,n}^4)} \right)} \right) - (1 + \lambda_i(t)) \\ &\times \left(\frac{3\alpha_{i,n}^2 E_{i,n}^4 z_{i,n}^2 \dot{z}_{i,n} + \alpha_{i,n}^2 z_{i,n}^6 \dot{z}_{i,n}}{\delta_i (E_{i,n}^4 - z_{i,n}^4)^2 \cosh^2 \left(\frac{z_{i,n}^3 \alpha_{i,n}}{\delta_i (E_{i,n}^4 - z_{i,n}^4)} \right)} + \frac{3\varphi_{i,n}^2 E_{i,n}^4 z_{i,n}^2 \dot{z}_{i,n} + \varphi_{i,n}^2 z_{i,n}^6 \dot{z}_{i,n}}{\delta_i (E_{i,n}^4 - z_{i,n}^4)^2 \cosh^2 \left(\frac{z_{i,n}^3 \varphi_{i,n}}{\delta_i (E_{i,n}^4 - z_{i,n}^4)} \right)} \right). \quad (65) \end{aligned}$$

Based on (65), we know that $\dot{v}_i(t)$ represents a continuous function. There has a positive parameter \mathbb{Q} with $|\dot{e}_i(t)| < \mathbb{Q}$, $e_i(\bar{t}_\kappa) = 0$ and $\lim_{t \rightarrow \bar{t}_{\kappa+1}} e_i(t) > \lambda_i(\bar{t}_{\kappa+1}) |u_i(t)| + \mu_i > 0$. Therefore, the minimum triggering interval t_{\min} satisfies $\bar{t}_{\kappa+1} - \bar{t}_\kappa \geq t_{\min} > \frac{\mu_i}{\mathbb{Q}}$, which proves the exclusion of Zeno behavior. \square

Remark 1. From [59], the command filter (8) is stable, and the command filter output signal $\partial_{i,\vartheta}$ is bounded such that $|\partial_{i,\vartheta}| < \bar{\partial}_{i,\vartheta}$. It is worth noting that we have made modifications to the error compensation system (10) to make the algorithm simpler. The system remains stable, and the error compensation signal $\gamma_{i,\vartheta}$ is bounded such that $|\gamma_{i,\vartheta}| < \bar{\gamma}_{i,\vartheta}$, where $\bar{\partial}_{i,\vartheta}$ and $\bar{\gamma}_{i,\vartheta}$ are positive constants, $\vartheta = 1, 2, \dots, n$.

The following demonstrates that the full state constraints of MASs do not be violated. According to (9), we can obtain

$$|s_{i,\vartheta}| < |E_{i,\vartheta}| + \bar{\gamma}_{i,\vartheta}. \quad (66)$$

According to Assumption 2, one has $|y_0| < \bar{y}_0$, where \bar{y}_0 is a positive constant. Substituting (7) into (66), one has

$$\begin{aligned} |x_{i,1}| &< \frac{|E_{i,1}| + |\mathfrak{S}_i| + \bar{\gamma}_{i,1} + \bar{h}_i \bar{y}_0 + \left| \sum_{i=1}^N \rho_{i,i} y_i \right|}{d_i + \bar{h}_i}, \\ |x_{i,\vartheta}| &< \bar{\partial}_{i,\vartheta} + \bar{\gamma}_{i,\vartheta} + |E_{i,\vartheta}| \end{aligned} \quad (67)$$

where $\vartheta = 1, 2, \dots, n$, $\mathfrak{S}_i = \sum_{i=1}^N \rho_{i,i} \mathfrak{S}_{i,i} + \bar{h}_i \mathfrak{S}_{i,0}$.

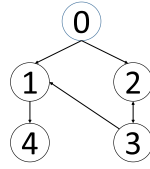


Figure 2. Communication topology

Table 1. Triggering times in 50 seconds of different event-triggering control strategies

Triggering times	Follower 1	Follower 2	Follower 3	Follower 4
Fixed threshold event triggering control	1931	1329	2694	2977
Relative threshold event triggering control	984	922	1373	1165
DET control	910	692	1179	1080

From (67), we define functions $\bar{H}_{i,1}$ and $\bar{H}_{i,\vartheta}$ satisfy $\frac{|E_{i,1}|+|\Im_i|+\bar{\gamma}_{i,1}+h_i\bar{y}_0+|\sum_{i=1}^N \rho_{i,\vartheta} y_i|}{d_i+h_i} < \bar{H}_{i,1}$, $\bar{\partial}_{i,\vartheta} + \bar{\gamma}_{i,\vartheta} + |E_{i,\vartheta}| < \bar{H}_{i,\vartheta}$, respectively. We can get $|x_{i,1}| < \bar{H}_{i,1}$ and $|x_{i,\vartheta}| < \bar{H}_{i,\vartheta}$, which indicates that the full state constraints are not transgressed.

Remark 2. The design parameters adhere to several guidelines. The appropriate design parameters are selected such that $C_1 > 0$. Therefore, $c_{i,\vartheta} > 0$ and $H_{i,\vartheta} > 0$ are selected to ensure system stability. Then, another parameter $E_{i,\vartheta}$ satisfies $|z_{i,\vartheta}| < |E_{i,\vartheta}|$ to ensure that all states of the closed-loop system are constrained. It is worth noting that the larger the value of $c_{i,\vartheta}$, the better the system performance, but the computation time also increases. Therefore, it is important to choose appropriate parameters to meet the requirements of the system.

5 Simulation

To illustrate the feasibility of the proposed control strategy, a numerical simulation example is provided. In Figure 2, the communication topology diagram with a leader and four followers is displayed.

From Figure 2, we know that the expansion adjacency matrix is $\bar{Q} = [1, 1, 0, 0]$ and the adjacency matrix Q is given as

$$Q = \begin{bmatrix} 0 & 0 & 1 & 0 \\ 0 & 0 & 1 & 0 \\ 0 & 1 & 0 & 0 \\ 1 & 0 & 0 & 0 \end{bmatrix}.$$

The follower dynamic model is given as

$$\begin{aligned} dx_{i,1} &= (x_{i,2} + f_{i,1}(\bar{x}_{i,1})) dt + g_{i,1}^T(\bar{x}_{i,1}) d\omega, \\ dx_{i,2} &= (u_i + f_{i,2}(\bar{x}_{i,2})) dt + g_{i,2}^T(\bar{x}_{i,2}) d\omega, \\ y_i &= x_{i,1}, \end{aligned}$$

where $f_{i,1}(\bar{x}_{i,1}) = x_{i,1} \sin(t)$, $f_{i,2}(\bar{x}_{i,2}) = 0.5x_{i,1}x_{i,2} \cos(t)$, $i = 1, 2, 3, 4$.

The control input $u_0(t)$ of leader (2) is designed as follows:

$$u_0(t) = \begin{cases} 0.3 \sin(1.2t), & 0 \leq t < 15, \\ 0.5 \cos(t) \sin(0.1t), & 15 \leq t < 30, \\ 0.2 \sin(0.4t), & 30 \leq t \leq 50. \end{cases}$$

The main design parameters are selected as $\beta_i = 0.03$, $\mu_i = 0.01$, $L_{i,1} = 75$, $R_{i,1} = 3$, $c_{i,1} = 75$, $c_{i,2} = 85$, $k_{i,1} = 0.3$, $k_{i,2} = 0.12$, $\tau_{i,1} = \tau_{i,2} = 2$, $H_{i,1} = H_{i,2} = 1.2$, $\varphi_{i,2} = 2$, $\epsilon_{i,1} = \epsilon_{i,2} = 1.5$ and

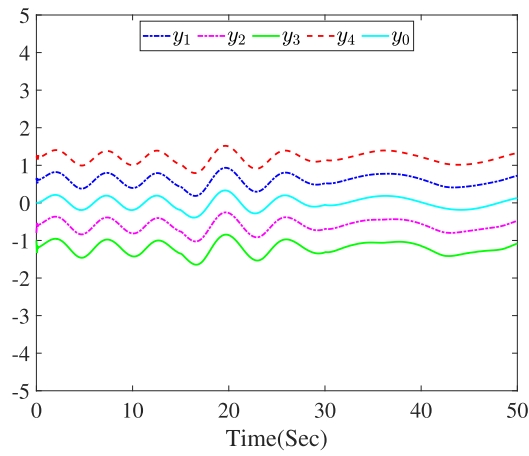


Figure 3. Trajectories of followers y_i ($i = 1, 2, 3, 4$) and Leader y_0

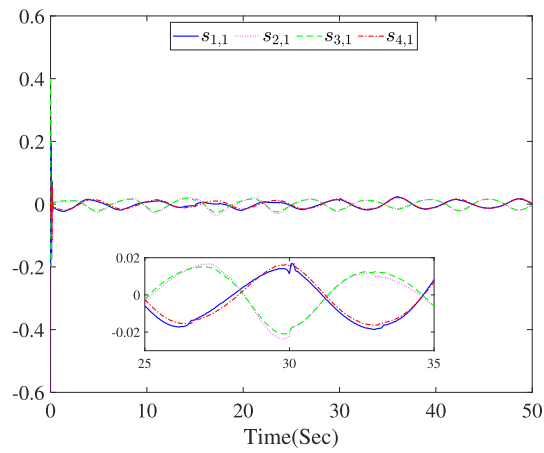


Figure 4. Curves of formation errors $s_{i,1}$ ($i = 1, 2, 3, 4$)

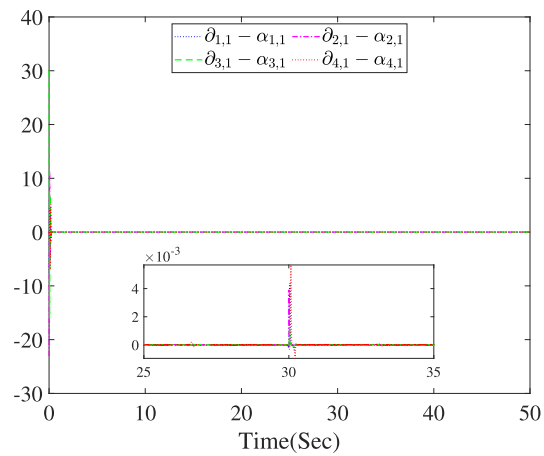


Figure 5. Curves of filtering errors $\partial_{i,1} - \alpha_{i,1}$ ($i = 1, 2, 3, 4$)

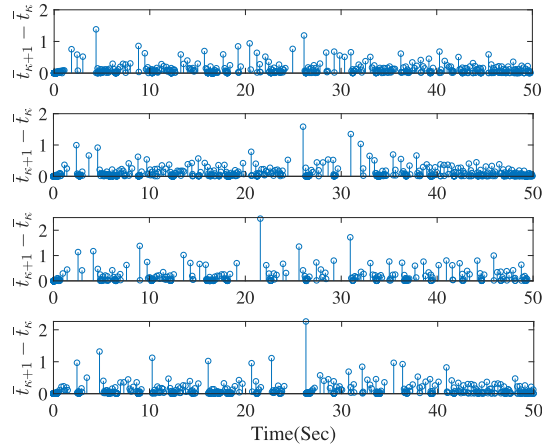


Figure 6. Interevent times of control signals

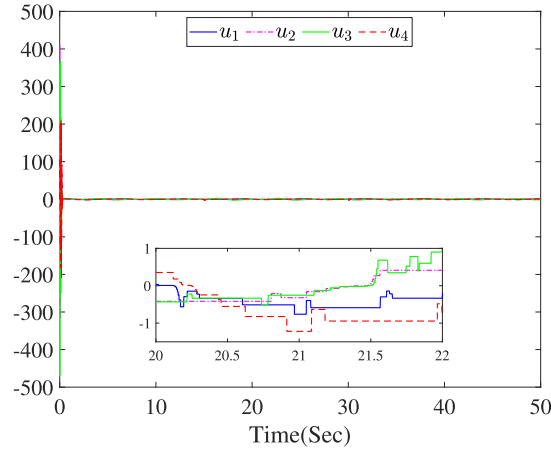


Figure 7. Curves of control inputs $u_i (i = 1, 2, 3, 4)$

the constraint parameters of the compensating error are $E_{i,1} = 0.8$ and $E_{i,2} = 0.5$, the initial values of MASs are designed as $x_{1,1}(0) = 0.6$, $x_{2,1}(0) = -0.8$, $x_{3,1}(0) = -1$, $x_{4,1}(0) = -1.2$ and $x_{i,2}(0) = 0$. According to the communication topology diagram. The formation distances are designed such that $\mathfrak{S}_{1,0} = 0.6$, $\mathfrak{S}_{1,3} = 1.8$, $\mathfrak{S}_{2,0} = -0.6$, $\mathfrak{S}_{2,3} = 0.6$, $\mathfrak{S}_{3,2} = -0.6$, $\mathfrak{S}_{4,1} = 0.6$. Figure 3 shows the formation trajectory of the MASs under state constraints. The formation error is displayed in Figure 4. Figure 5 displays the error curves of filter output signals and virtual control signals. Figure 6 displays the time intervals of triggering events with the followers $i (i = 1, 2, 3, 4)$ from top to bottom. In Table 1, compared with two different event-triggered control methods, the results show that the DET control scheme obtains fewer trigger times, which proves that the proposed control method can reduce the consumption of communication resources more efficiently. The input signals of followers are depicted in Figure 7.

6 Conclusion

The formation control problem for a category of HiTL stochastic nonlinear MASs with full state constraints has been addressed. A DET mechanism has been presented to effectively reduce the communication burden. A BLF has been constructed to address the full state constraints problem. Under the backstepping control framework, the RBF NNs and command filter have been introduced to address the challenges with unknown nonlinear terms and “explosion of complexity”, respectively. Moreover, a filtering error compensation system has been designed to compensate for errors caused by the command filter. Through the provision of the control signal to the leader, the designed distributed formation controller

has guaranteed that all followers can achieve the desired formation trajectory and all signals in the MASs have been SGUUB in probability. Finally, the simulation example has validated the effectiveness of the designed control method.

Conflict of Interest

The authors declare that they have no conflict of interest.

Data Availability

No data are associated with this article.

Authors' Contributions

Yonghua Peng constructed and wrote the article, Guohuai Lin participated in writing and refined the language, and Guangdeng Chen and Hongyi Li sorted out and analyzed the research results and discussed the latest developments.

Acknowledgements

We thank all editors and reviewers who helped us improve this paper.

Funding

This work was supported in part by the National Natural Science Foundation of China (62121004, 62033003, 61973091, 62203119), the Local Innovative and Research Teams Project of Guangdong Special Support Program (2019BT02X353), the Natural Science Foundation of Guangdong Province (2023A1515011527, 2022A1515011506), and the China National Postdoctoral Program (BX20220095, 2022M710826).

References

- [1] Yao D, Li H and Lu R et al. Event-triggered guaranteed cost leader-following consensus control of second-order nonlinear multiagent systems. *IEEE Trans Syst Man Cybern: Syst* 2022; **52**: 2615–24.
- [2] Fu J, Lv Y and Yu W. Robust adaptive time-varying region tracking control of multi-robot systems. *Sci Chin Inf Sci* 2023; **66**: 159202.
- [3] Sun J, Zhou H and Xi H et al. Adaptive design of experiments for safety evaluation of automated vehicles. *IEEE Trans Intell Transp Syst* 2022; **23**: 14497–508.
- [4] Pan Y, Li Q and Liang H et al. A novel mixed control approach for fuzzy systems via membership functions online learning policy. *IEEE Trans Fuzzy Syst* 2022; **30**: 3812–22.
- [5] Ren H, Ma H and Li H et al. Adaptive fixed-time control of nonlinear MASs with actuator faults. *IEEE/CAA J Autom Sin* 2023; **10**: 1252–62.
- [6] Liu Y, Yao D and Wang L et al. Distributed adaptive fixed-time robust platoon control for fully heterogeneous vehicles. *IEEE Trans Syst Man Cybern: Syst* 2023; **53**: 264–74.
- [7] Li X, Wen C and Chen C. Adaptive formation control of networked robotic systems with bearing-only measurements. *IEEE Trans Cybern* 2021; **51**: 199–209.
- [8] Dai S L, He S and Cai H et al. Adaptive leader-follower formation control of underactuated surface vehicles with guaranteed performance. *IEEE Trans Syst Man Cybern: Syst* 2022; **52**: 1997–2008.
- [9] Zhang D, Tang Y and Zhang W et al. Hierarchical design for position-based formation control of rotorcraft-like aerial vehicles. *IEEE Trans Control Netw Syst* 2020; **7**: 1789–800.
- [10] Van Vu D, Trinh MH and Nguyen PD et al. Distance-based formation control with bounded disturbances. *IEEE Control Syst Lett* 2021; **5**: 451–6.
- [11] Li R, Zhang L and Han L et al. Multiple vehicle formation control based on robust adaptive control algorithm. *IEEE Intell Transp Syst Mag* 2017; **9**: 41–51.
- [12] Li J, Fang Y and Cheng H et al. Large-scale fixed-wing UAV swarm system control with collision avoidance and formation maneuver. *IEEE Syst J* 2023; **17**: 744–55.
- [13] Dong X, Li Y and Lu C et al. Time-varying formation tracking for UAV swarm systems with switching directed topologies. *IEEE Trans Neural Netw Learn Syst* 2019; **30**: 3674–85.
- [14] Guo Z, Li H and Ma H et al. Distributed optimal attitude synchronization control of multiple QUAVs via adaptive dynamic programming. *IEEE Trans Neural Netw Learn Syst* 2022, doi: [10.1109/TNNLS.2022.3224029](https://doi.org/10.1109/TNNLS.2022.3224029).
- [15] Ding SX. A note on diagnosis and performance degradation detection in automatic control systems towards functional safety and cyber security. *Secur Saf* 2022; **1**: 2022004.
- [16] Liu Z, Gao H and Yu X et al. B-spline wavelet neural network-based adaptive control for linear motor-driven systems via a novel gradient descent algorithm. *IEEE Trans Ind Electron* 2023; **71**: 1896–905.
- [17] Ren H, Ma H and Li H et al. A disturbance observer based intelligent control for nonstrict-feedback nonlinear systems. *Sci China Technol Sci* 2022; **66**: 456–67.
- [18] Sun J, Zhang H and Wang Y et al. Fault-tolerant control for stochastic switched IT2 fuzzy uncertain time-delayed nonlinear systems. *IEEE Trans Cybern* 2022; **52**: 1335–46.
- [19] Li Y, Min X and Tong S. Observer-based fuzzy adaptive inverse optimal output feedback control for uncertain nonlinear systems. *IEEE Trans Fuzzy Syst* 2021; **29**: 1484–95.
- [20] Hou M, Shi W and Fang L et al. Adaptive dynamic surface control of high-order strict feedback nonlinear systems with parameter estimations. *Sci China Inf Sci* 2023; **66**: 159203.

- [21] Gao H, Li Z and Yu X et al. Hierarchical multiobjective heuristic for PCB assembly optimization in a beam-head surface mounter. *IEEE Trans Cybern* 2022; **52**: 6911–24.
- [22] Gao S, Zhang H and Wang Z et al. Optimal injection attack strategy for cyber-physical systems: a dynamic feedback approach. *Secur Saf* 2022; **1**: 2022005.
- [23] Shi P, Sun W and Yang X et al. Master-slave synchronous control of dual-drive gantry stage with cogging force compensation. *IEEE Trans Syst Man Cybern: Syst* 2023; **53**: 216–25.
- [24] Zeng HB, He Y and Teo KL. Monotone-delay-interval-based Lyapunov functionals for stability analysis of systems with a periodically varying delay. *Automatica* 2022; **138**: 110030.
- [25] Zheng X, Li H and Ahn CK et al. NN-based fixed-time attitude tracking control for multiple unmanned aerial vehicles with nonlinear faults. *IEEE Trans Aerosp Electron Syst* 2022; **59**: 1738–48.
- [26] Ren H, Wang Y and Liu M et al. An optimal estimation framework of multi-agent systems with random transport protocol. *IEEE Trans Signal Process* 2022; **70**: 2548–59.
- [27] Zhang H, Zhao X and Wang H et al. Adaptive tracking control for output-constrained switched MIMO pure-feedback nonlinear systems with input saturation. *J Syst Sci Complex* 2023; **36**: 960–84.
- [28] Liu Z, Lin W and Yu X et al. Approximation-free robust synchronization control for dual-linear-motors-driven systems with uncertainties and disturbances. *IEEE Trans Ind Electron* 2022; **69**: 10500–9.
- [29] Ma L, Zhu F and Zhao X. Human-in-the-loop consensus control for multiagent systems with external disturbances. *IEEE Trans Neural Netw Learn Syst* 2023, doi: [10.1109/TNNLS.2023.3246567](https://doi.org/10.1109/TNNLS.2023.3246567).
- [30] Feng L, Wiltche C and Humphrey L et al. Synthesis of human-in-the-loop control protocols for autonomous systems. *IEEE Trans Autom Sci Eng* 2016; **13**: 450–62.
- [31] Koru AT, Yucelen T and Sipahi R et al. Stability of human-in-the-loop multiagent systems with time delays. In: 2019 American Control Conf (ACC). IEEE, 2019, 4854–9.
- [32] Lin G, Li H and Ma H et al. Distributed containment control for human-in-the-loop MASs with unknown time-varying parameters. *IEEE Trans Circuits Syst I Reg Papers* 2022; **69**: 5300–11.
- [33] Wu HN. Online learning human behavior for a class of human-in-the-loop systems via adaptive inverse optimal control. *IEEE Trans Human-Machine Syst* 2022; **52**: 1004–14.
- [34] Lin G, Li H and Ahn CK et al. Event-based finite-time neural control for human-in-the-loop UAV attitude systems. *IEEE Trans Neural Netw Learn Syst* 2022, doi: [10.1109/TNNLS.2022.3166531](https://doi.org/10.1109/TNNLS.2022.3166531).
- [35] Su H, Cheng B and Li Z. Cooperative output regulation of heterogeneous systems over directed graphs: a dynamic adaptive event-triggered strategy. *J Syst Sci Complex* 2023; **36**: 909–21.
- [36] Sun W, Shen JX and Wang K et al. Motor control application of fixed-sampling-interval and fixed-depth moving average filters. *IEEE Trans Ind Appl* 2016; **52**: 1831–41.
- [37] Baek S, Cho Y and Lai JS. Average periodic delay-based frequency adaptable repetitive control with a fixed sampling rate and memory of single-phase PFC converters. *IEEE Trans Power Electron* 2021; **36**: 6572–85.
- [38] Wang X, Sun J and Wang G et al. Data-driven control of distributed event-triggered network systems. *IEEE/CAA J Autom Sinica* 2023; **10**: 351–64.
- [39] Chen G, Liu Y and Yao D et al. Event-triggered tracking control of nonlinear systems under sparse attacks and its application to rigid aircraft. *IEEE Trans Aerosp Electron Syst* 2023; **59**: 4640–50.
- [40] Cao L, Cheng Z and Liu Y et al. Event-based adaptive NN fixed-time cooperative formation for multiagent systems. *IEEE Trans Neural Netw Learn Syst* 2022, doi: [10.1109/TNNLS.2022.3210269](https://doi.org/10.1109/TNNLS.2022.3210269).
- [41] Shangguan XC, Zhang CK and He Y et al. Robust load frequency control for power system considering transmission delay and sampling period. *IEEE Trans Ind Inf* 2021; **17**: 5292–303.
- [42] Li H, Luo J and Ma H et al. Observer-based event-triggered iterative learning consensus for locally lipschitz nonlinear MASs. *IEEE Trans Cogn Dev Syst* 2023, doi: [10.1109/TCDS.2023.3274794](https://doi.org/10.1109/TCDS.2023.3274794).
- [43] Yao D, Li H and Shi Y. Adaptive event-triggered sliding-mode control for consensus tracking of nonlinear multiagent systems with unknown perturbations. *IEEE Trans Cybern* 2023; **53**: 2672–84.
- [44] Li Y, Li YX and Tong S. Event-based finite-time control for nonlinear multiagent systems with asymptotic tracking. *IEEE Trans Autom Control* 2023; **68**: 3790–7.
- [45] Ren H, Cheng Z and Qin J et al. Deception attacks on event-triggered distributed consensus estimation for nonlinear systems. *Automatica* 2023; **154**: 111100.
- [46] Chen L, Wang Y and Hou Z G et al. Sampled-data based average consensus of second-order integral multi-agent systems: Switching topologies and communication noises. *Automatica* 2013; **49**: 1458–64.
- [47] Bernuau E, Moulay E and Coirault P et al. Practical consensus of homogeneous sampled-data multiagent systems. *IEEE Trans Autom Control* 2019; **64**: 4691–7.
- [48] Qiu J, Sun K and Wang T et al. Observer-based fuzzy adaptive event-triggered control for pure-feedback nonlinear systems with prescribed performance. *IEEE Trans Fuzzy Sys* 2019; **27**: 2152–62.
- [49] Ma H, Li H and Lu R et al. Adaptive event-triggered control for a class of nonlinear systems with periodic disturbances. *Sci China Inf Sci* 2020; **63**: 150212.
- [50] Liu L, Liu Y J and Tong S et al. Relative threshold-based event-triggered control for nonlinear constrained systems with application to aircraft wing rock motion. *IEEE Trans Ind Inf* 2022; **18**: 911–21.
- [51] Wang L and Chen CLP. Reduced-order observer-based dynamic event-triggered adaptive NN control for stochastic nonlinear systems subject to unknown input saturation. *IEEE Trans Neural Netw Learn Syst* 2021; **32**: 1678–90.
- [52] Cao L, Pan Y and Liang H et al. Observer-based dynamic event-triggered control for multiagent systems with time-varying delay. *IEEE Trans Cybern* 2023; **53**: 3376–87.
- [53] Tarczewski T and Grzesiak LM. Constrained state feedback speed control of PMSM based on model predictive approach. *IEEE Trans Ind Electron* 2016; **63**: 3867–75.
- [54] Zhang T, Xia M and Yi Y. Adaptive neural dynamic surface control of strict-feedback nonlinear systems with full state constraints and unmodeled dynamics. *Automatica* 2017; **81**: 232–9.

- [55] Wang T, Ma M and Qiu J et al. Event-triggered adaptive fuzzy tracking control for pure-feedback stochastic nonlinear systems with multiple constraints. *IEEE Trans Fuzzy Syst* 2021; **29**: 1496–506.
- [56] Ma H, Ren H and Zhou Q et al. Observer-based neural control of N -link flexible-joint robots. *IEEE Trans Neural Netw Learn Syst* 2022, doi: [10.1109/TNNLS.2022.3203074](https://doi.org/10.1109/TNNLS.2022.3203074).
- [57] Sun Y, Chen B and Lin C et al. Adaptive neural control for a class of stochastic nonlinear systems by backstepping approach. *Inf Sci* 2016; **369**: 748–64.
- [58] Chen B, Liu XP and Ge SS et al. Adaptive fuzzy control of a class of nonlinear systems by fuzzy approximation approach. *IEEE Trans Fuzzy Syst* 2012; **20**: 1012–21.
- [59] Yu J, Shi P and Zhao L. Finite-time command filtered backstepping control for a class of nonlinear systems. *Automatica* 2018; **92**: 173–80.



Yonghua Peng received a B.S. degree in Information Engineering from Henan University of Science and Technology, Luoyang, China, in 2022. He is currently pursuing an M.S. degree in control science and engineering at Guangdong University of Technology, Guangzhou, China. His research interests include human-in-the-loop control, formation control, and event-triggered control for nonlinear multi-agent systems.



Guohuai Lin received a B.S. degree in Electrical Engineering and Automation from the Guangdong University of Petrochemical Technology, Maoming, China, in 2018. He is currently pursuing his Ph.D. degree in Control Science and Engineering at Guangdong University of Technology, Guangzhou, China. His current research interests include adaptive control and human-in-the-loop control for multi-agent systems.



Guangdeng Chen received a B.S. degree from the Guangdong University of Petrochemical Technology, Maoming, China, in 2018, and a M.S. degree in control science and engineering from the Guangdong University of Technology, Guangzhou, China, in 2021, where he is currently pursuing the Ph.D. degree in control science and engineering. His research interests include event-triggered control, nonlinear systems, and cyber-physical systems.



Hongyi Li (Senior Member, IEEE) received a Ph.D. degree in intelligent control from the University of Portsmouth, Portsmouth, U.K., in 2012. He is currently a professor at the Guangdong University of Technology, Guangdong, China. His research interests include intelligent control, cooperative control, sliding mode control, and their applications.